AUV Networking: Addressing Positional Uncertainty in Underwater Environments

Shuai Dong
Computer Science
University of Alabama
Tuscaloosa, Alabama, US
sdong7@crimson.ua.edu

Bineet Ghosh
Computer Science
University of Alabama
Tuscaloosa, Alabama, US
bineet@ua.edu

Xiaoyan Hong
Computer Science
University of Alabama
Tuscaloosa, Alabama, US
hxy@cs.ua.edu

Beichen Yang
Computer Science
University of Alabama
Tuscaloosa, Alabama, US
byang12@crimson.ua.edu

Abstract

Positional uncertainty in underwater Autonomous Underwater Vehicle (AUV) networks can lead to inefficient communication and more energy consumption. This paper proposes the Uncertainty and Lifetime Aware Vector-Based Forwarding (UL-VBF) protocol, which enhances the original Vector-Based Forwarding (VBF) protocol by calculating the waiting times with variables counting for uncertainty. Simulations in AquaSim compare UL-VBF with the original VBF and the worst case of VBF under uncertainty. Results show that UL-VBF reduces energy consumption deviation by 35%, average end-to-end delay by 23%, and extends network lifetime by 24% compared to VBF under worst-case uncertainty conditions. Meanwhile, UL-VBF maintains packet delivery ratios comparable to ideal scenarios. The results show the effectiveness of the proposed method in handling uncertain in underwater environments.

CCS Concepts

• **Networks** → **Network protocol design**.

Keywords

Positional Uncertainty, Underwater AUV Networks, Underwater Routing protocols, Network Lifetime, Energy Consumption

ACM Reference Format:
Shuai Dong, Bineet Ghosh, Xiaoyan Hong, and Beichen Yang. 2024. AUV Networking: Addressing Positional Uncertainty in Underwater Environments. In *The 18th ACM International Conference on Underwater Networks & Systems (WUWNET '24), October 28–31, 2024, Sibenik, Croatia.* ACM, New York, NY, USA, 5 pages. https://doi.org/10.1145/3699432.3699498

1 Introduction

Autonomous Underwater Vehicles (AUVs) have become indispensable in various water-related domains, including ocean exploration and environmental monitoring [5]. These applications require networked AUVs with consistent and reliable underwater communication. However, the underwater environment's uncertainty and dynamism pose significant challenges. Variations in temperature, salinity, and depth variations can affect sound speed, causing transmission delays. High-frequency signals attenuate rapidly, while low-frequency signals scatter, degrading quality [2]. Dynamic ocean currents further complicate signal propagation [9]. These factors increase the complexity of maintaining effective communication and lead to inefficient energy consumption as AUVs expend more power to maintain connectivity in unpredictable conditions.

Several multi-hop routing protocols have been developed to enhance energy efficiency in underwater networks. A few examples are within the VBF protocol group. The basic VBF protocol optimizes energy usage by creating a virtual pipe between the source and destination, which limits the number of nodes involved in forwarding so as to conserve energy [11]. Only the nodes within the pipe participate in message forwarding. In this protocol, a waiting time is used such that a node holding a message has to delay per the set time before re-broadcasting it. Building on this, the Localized Energy-Aware VBF (LE-VBF) protocol introduces an energy factor into the waiting time calculation. It accounts for nodes' residual energy so to prevent early depletion [10]. Another protocol, Hop-by-Hop VBF (HH-VBF), applies the pipe line concept to each routing hop. The per-hop virtual pipes allow nodes to make adaptive forwarding decisions based on their current locations, thereby enhancing energy efficiency [8].

However, these protocols don't account for node position uncertainty, a critical issue in underwater environments. Factors like water property variations, equipment reliability, and dynamic conditions [3][6] affect positional accuracy, leading to localization errors. These uncertainties can cause misestimations in VBF protocols, resulting in incorrect waiting times, inefficient routing, and increased energy consumption. In LE-VBF, inaccurate locations may lead to poor node selection and uneven energy use. For HH-VBF, positional uncertainties make per-hop virtual pipes unreliable, potentially increasing packet loss and communication overhead.

To address these challenges introduced by positional uncertainty, this paper proposes an innovated underwater routing protocol,

WUWNET '24, October 28–31, 2024, Sibenik, Croatia

ACM ISBN 979-8-4007-1160-2/24/10
https://doi.org/10.1145/3699432.3699498

namely UL-VBF. Our proposed protocol builds on top of the original VBF routing protocol. It uses the pipe line design and the waiting time as core routing principles. Additionally, an energy factor based on the residual energy is also integrated into calculation of the waiting time. Such waiting time calculation can be directly performed in the original VBF protocol since the exact three dimensional coordinates of all the nodes are assumed to be known by the protocol. However due to the uncertainty, precise coordinates are hard to acquire. In our proposed UL-VBF protocol, instead using exact coordinates, three-dimensional ranges are used to represent the obscure node positions. Accordingly, the calculation process of waiting time is based on nodes' 3D ranges. Tools of interval arithmetic and Gurobi [1, 4] are used in the calculation of the waiting time. The tools help in handling the complexity of the problem and ensure reliable outputs. The output of this calculation process is ranges of waiting time for all the nodes. It is interesting to mention that the two tools offer different waiting time ranges outputs. Each of the two results can be used in derive waiting time depending on the rational that a researcher wants to follow. In the paper, the cases will be discussed, a couple of which are used in the evaluation.

The effectiveness of UL-VBF and related protocols are evaluated using simulator AquaSim[7]. Network performance metrics, such as network lifetime, packet delivery ratio, energy consumption, and average end-to-end delay are used. The results show UL-VBF enhances network performance compared to the worst-case scenario under positional uncertainties. Specifically, UL-VBF reduces energy deviation, demonstrating more balanced energy consumption across nodes. It also improves the average end-to-end delay, ensuring faster data transmission. The packet delivery ratio of UL-VBF remains consistent with ideal conditions, showing robustness in maintaining high reliability. Moreover, UL-VBF extends network lifetime by efficiently managing energy consumption.

The rest of the paper is organized as: Section II introduces the proposed UL-VBF protocol, followed by Section III describing the evaluation. Conclusion is given in Section IV.

2 Uncertainty and Lifetime in UL-VBF

UL-VBF builds on general protocol design of VBF with a new factor concerning energy and more importantly, factors expressing uncertainties and a method handling the expressions. The following subsections start with a brief description of the original VBF protocol, especially the waiting time calculation. It is followed by adding an energy factor and further factoring uncertainties into the calculation. Then, methods to derive the desired waiting times will be given.

2.1 Network Model

VBF uses a pipeline to guide waiting time calculation before packet transmission. Fig 1 shows a typical network scenario with source node O, sink node T, current node pos (coordinates $(pos.x, pos.y, pos.z)$), and other nodes f_i. The direct line $\overline{OT}$ forms the center of a virtual pipe with width L. Communication range R is the maximum distance for node communication. p is the projection distance from pos to $\overline{OT}$, d is the Euclidean distance between pos and the previous-hop node, and θ is the angle between the lines connecting the previous-hop node to the sink and to pos.

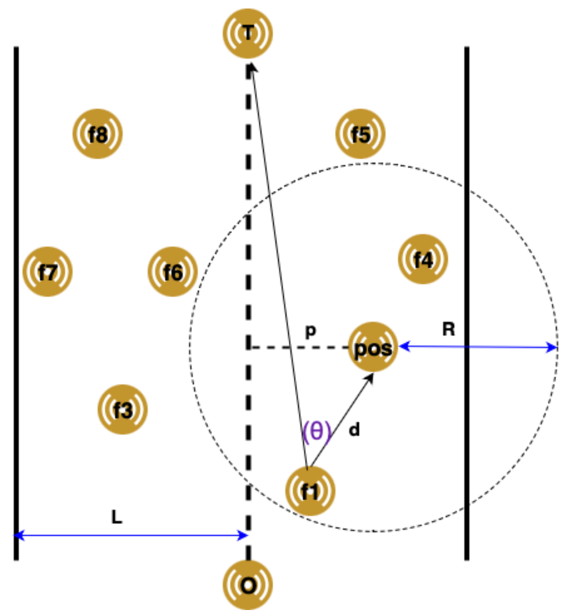

Figure 1: An Example of a Network Scenario

2.2 Energy Factor in Waiting Time

The waiting time (W) in the original VBF protocol is calculated based on projection p, distance d, and angle θ with normalization, according to the formula in [11]. Each node, upon receiving a message, will defer for the waiting time before deciding on whether or not the message needs to be sent.

$$\mathrm{W} = \left(\frac{p}{L}\right) + \left(\frac{R - d \cdot \cos(\theta)}{R}\right). \tag{1}$$

In UL-VBF, energy consumption factor is added, which takes in the current consumed energy (e_{c_i}) and the initial energy (e_{i_i}) of each node. The modified calculation for waiting time of node i (W_i) becomes:

$$\mathrm{W}_i = \left(\frac{p_i}{L}\right) + \left(\frac{R - d_i \cdot \cos(\theta_i)}{R}\right) + \frac{e_{c_i}}{e_{i_i}} \tag{2}$$

Nodes with higher $\frac{e_{c_i}}{e_{i_i}}$ values are those have more residual energy percentage wise, which leads to longer waiting times, reducing their chances in participating in forwarding. In contrast, those consumed less, i.e., having higher residual energy will have short waiting time. They will have higher priority in having the chance of sending messages. The use of normalized value as the energy factor helps to prevent early energy depletion of the nodes in strategic locations, which in term, help balancing energy consumption across the network.

2.3 Integrate Uncertainty in UL-VBF

In UL-VBF, uncertainty in perceived positions are the most concerned. Positional measurements of AUVs are subject to uncertainties due to current, or other factors. To account for this, a noise range for each positional dimension is considered. The coordinates are then expressed as $pos.x \pm \Delta$, $pos.y \pm \Delta$, and $pos.z \pm \Delta$, where $\Delta \in [a, b]$. For simplicity, the range is the same for all the three dimensions. As an example, possible values of the dimension x of node pos falls within in the range of $pos.x - \Delta \leq pos.x \leq pos.x + \Delta$.

The positional uncertainty impacts the calculations of p, d, and θ and all subsequent calculations, altering the assumed exact positions to a range that reflects realistic operational conditions. With the noise range added to position, variables p, d, and θ should be revised to incorporate the associated range. The resulting waiting time will also be a value falling within a range. However, introducing a range into multiple variables pose challenges in solving them for a single output of the waiting time at each node. In the following, the equations where positions are used with uncertainties are described. Methods to solve them for the waiting time will be given in the follow subsection. For easy expression, the notation of Δ is omitted in all the coordinate variables of x, y, z respectively. Notations t, o, pos, f, refer to the nodes T (sink), O (source), current node, and the previous hop. The projection distance p from node pos to the center line $\overline{OT}$ is calculated by obtaining $\vec{a}$ and $\vec{b}$ first, then the cross product of $\vec{a} \times \vec{b}$. The latter is used in Eq.3. Specifically:

$$\vec{a} = (t.x - o.x, t.y - o.y, t.z - o.z)$$

$$\vec{b} = (pos.x - o.x, pos.y - o.y, pos.z - o.z)$$

$$p = \frac{\sqrt{(b_y a_z - b_z a_y)^2 + (b_z a_x - b_x a_z)^2 + (b_x a_y - b_y a_x)^2}}{\sqrt{(t.x - o.x)^2 + (t.y - o.y)^2 + (t.z - o.z)^2}} \quad (3)$$

The distance d is derived from the positional coordinates:

$$d = \sqrt{(pos.x - f.x)^2 + (pos.y - f.y)^2 + (pos.z - f.z)^2} \quad (4)$$

The angle θ is determined based on the positions of the current node pos, the previous node f and the sink t. The equations below show the calculations of two vectors and the cosine of θ.

$$\vec{u} = (pos.x - f.x, pos.y - f.y, pos.z - f.z)$$

$$\vec{v} = (t.x - f.x, t.y - f.y, t.z - f.z)$$

$$\cos(\theta) = \frac{\vec{u} \cdot \vec{v}}{|\vec{u}| \times |\vec{v}|} \quad (5)$$

where $|\vec{u}|$ is the magnitude of $\vec{u}$, $|\vec{v}|$ is the magnitude of $\vec{v}$.

2.4 Solving for Waiting Time

As described in previous subsection, the position of node pos falls into a 3-dimensional range due to uncertainty. Consequently, the values of projection p, distance d, and angle θ also fall into their corresponding ranges, per Equations 3, 4 and 5. Let notations of lb and ub represent lower bound and upper bound, $[p_{lb}, p_{ub}]$, $[d_{lb}, d_{ub}]$, and $[\theta_{lb}, \theta_{up}]$ are the ranges for p, d, and θ respectively. Solving Equations 3, 4 and 5 using interval arithmetic, these bounds can be obtained.

Similarly, Eq.2 shows that waiting time is calculated from three interdependent variables p, d, and θ, each falls in its corresponding uncertainty range. This creates a three-dimensional problem. Two methods can be used to solve it. The first method follows the interval arithmetic approach to obtain the lower and upper bounds for the waiting time, while the second method uses Gurobi, an optimization tool, to calculate the precise minimum and maximum waiting times. The range obtained via interval arithmetic usually is larger than the range determined by the minimum and maximum values from Gurobi. Choices on which method, or which value to use as waiting time depend on design goals.

In the following, Gurobi is used to calculate an exact waiting time. Gurobi handles the complexity by taking all constraints and variables simultaneously, producing the maximum or minimum waiting time. Assume each node prefers to be conservative in its energy consumption in terms of prolonging the network's lifetime, which is measured by the first depletion of a node's energy, the maximum value from Gurobi is used. As such, the frequency of packet transmissions from one node is minimized. The problem of finding the maximum waiting time $\mathcal{W}_{\max}$ for node pos given the uncertainties in positional coordinates $(pos.x, pos.y, pos.z)$ is defined to as follows:

$$\begin{aligned} \max \quad & \mathcal{W}_{max} = \mathrm{W}_{pos}(p, d, \theta) \\ \text{s.t.} \quad & p_{\text{lb}} \leq p \leq p_{\text{ub}}, \\ & d_{\text{lb}} \leq d \leq d_{\text{ub}}, \\ & \theta_{\text{lb}} \leq \theta \leq \theta_{\text{ub}}, \\ & p \text{ as in Eq. 3}, \\ & d \text{ as in Eq. 4}, \\ & \text{and } \theta \text{ as in Eq. 5}. \end{aligned} \quad (6)$$

We note that the formulation in Eq.6 computes the maximum wait time by maximizing W_{pos}. To compute the minimum wait time, one can simply modify the formulation in Eq.6 minimize W_{pos} without any change in the constraints.

3 Evaluations

This section evaluates our proposed UL-VBF protocol, comparing it with the original VBF (O-VBF) and a worst-case scenario calculated using interval arithmetic. We focus on four key performance metrics: packet delivery ratio (PDR), average end-to-end delay, energy consumption deviation, and network lifetime. Our analysis centers on how different waiting time calculations affect these metrics.

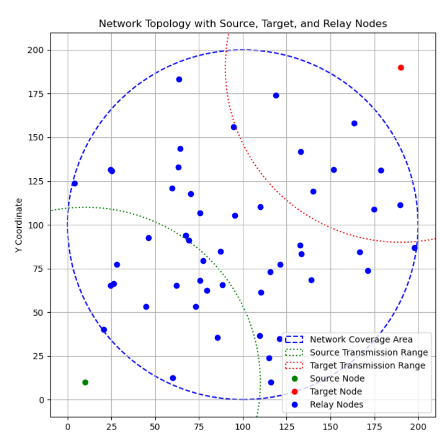

Figure 2: Example Network Topology with 50 Relay Nodes

3.1 Simulation Setup

We conduct simulations using the Aqua-Sim NG simulator for 1000 seconds, with 20 to 60 nodes in a circular area of 100 meters radius. A single source node broadcasts a 40-byte packet every five seconds to a single sink node at 10 kbps through relay nodes. Each node had a communication range of 100 meters, with transmission power set to 2W, reception power to 0.75W, and idle power to 0.008W. Initial node energy was 100 Joules. Figure 2 illustrates an example network topology with 50 relay nodes. The key difference between protocols lies in their waiting time calculations: O-VBF uses geographic distance and angle, ignoring energy and uncertainties; UL-VBF (Minimum) and (Maximum) employ minimum and maximum waiting times from Gurobi optimization, respectively, considering both energy and position uncertainties; the Worst Case scenario uses possible waiting times from interval arithmetic, representing extreme uncertainty conditions.

3.2 Results and Analysis

Figure 3 shows the PDR comparison, which is defined as the percentage of packets successfully delivered to their destination. Figure shows O-VBF and UL-VBF (Minimum) achieve 100% PDR across all node densities, while UL-VBF (Maximum) maintains 99% PDR. The Worst Case scenario shows variability from 90% to 99%, improving with increased node density.The high PDR of O-VBF and UL-VBF (Minimum) is primarily due to their shorter waiting times, which prioritize quick packet forwarding. O-VBF's waiting time calculation, based solely on geographic position, leads to faster forwarding but doesn't account for energy levels or uncertainties. UL-VBF (Minimum), while considering these factors, still maintains short waiting times, resulting in quick forwarding and high PDR. UL-VBF (Maximum)'s slightly lower PDR (99%) is a direct result of its longer waiting times, which are calculated to optimize energy efficiency and account for uncertainties. These longer waiting times occasionally lead to packet expiration, but the protocol still maintains a high PDR. The Worst Case scenario's lower and variable PDR illustrates the negative impact of extreme waiting times calculated under maximum uncertainty.

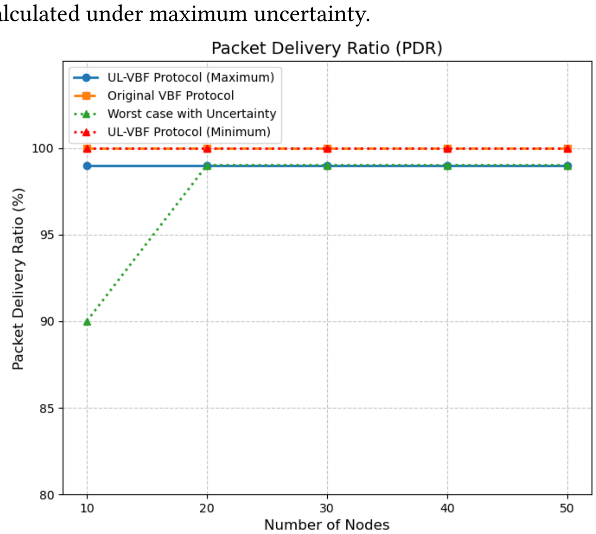

Figure 3: Packet Delivery Ratio Comparison

Figure 4 shows O-VBF has the lowest delay, followed by UL-VBF (Minimum), UL-VBF (Maximum), and the Worst Case scenario, reflecting the average time taken for a packet to traverse from the source to the sink. O-VBF's simplicity yields the lowest delay but ignores energy levels and uncertainties. UL-VBF (Minimum) slightly increases delay by incorporating energy and uncertainty considerations using minimum optimization values, balancing quick forwarding with improved management. UL-VBF (Maximum) uses of maximum waiting times from the optimization process. These longer waiting times allow for more consideration of energy levels and uncertainties at the cost of increased delay. The Worst Case scenario has the highest delay due to maximum waiting times under extreme uncertainty. UL-VBF (Maximum)'s delay is 19-23% lower than the worst case, demonstrating effective uncertainty management while maintaining reasonable delay times.

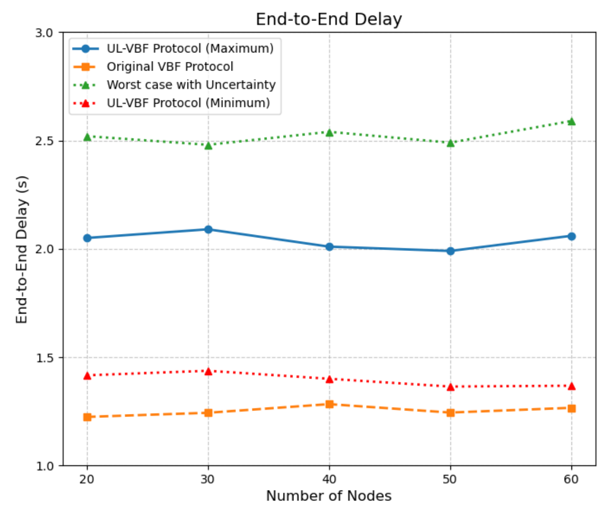

Figure 4: Average End-to-End Delay Comparison

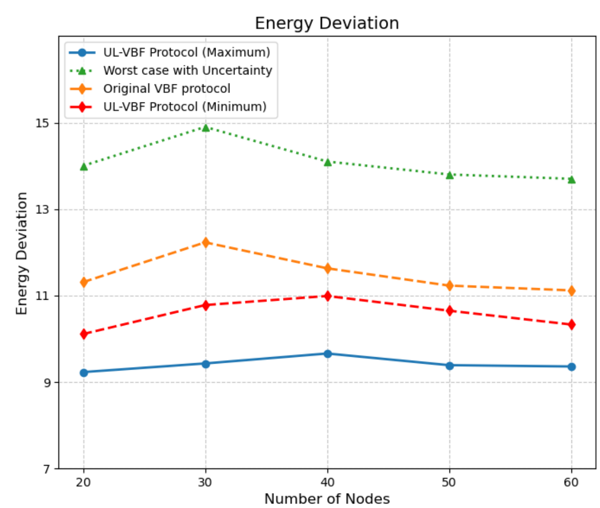

Figure 5: Energy Consumption Deviation Comparison

Figure 5 shows UL-VBF (Maximum) has the lowest energy deviation, followed by UL-VBF (Minimum), O-VBF, and the Worst Case scenario, reflecting standard deviation of residual energies recorded for each node during the simulation. O-VBF's higher deviation results from ignoring energy levels, overusing favorably positioned nodes. UL-VBF (Minimum) improves by incorporating energy considerations, but its use of minimum waiting times limits optimization. UL-VBF (Maximum) achieves the lowest deviation by using maximum waiting times, allowing more energy-aware routing decisions and balanced consumption. The Worst Case scenario's high deviation demonstrates how extreme uncertainty affects energy distribution. Notably, UL-VBF (Maximum)'s energy deviation is 32-35% lower than the worst case, highlighting its effectiveness in maintaining energy balance under high uncertainty.

Figure 6 shows that UL-VBF (Maximum) achieves the longest network lifetime, followed by O-VBF, UL-VBF (Minimum), and the Worst Case scenario. Network Life Time (NLT) refers to the duration of time the network remains operational. O-VBF's moderate network lifetime is a consequence of its waiting time calculation not considering energy levels. UL-VBF (Minimum), despite considering energy in its waiting time calculations, prioritizes quicker packet delivery. This results in a network lifetime similar to O-VBF, as the energy considerations are limited by the use of minimum waiting times. UL-VBF (Maximum) extends network lifetime by using maximum waiting times from its optimization process. The Worst Case scenario's short network lifetime illustrates how extreme uncertainty in waiting time calculations can lead to rapid energy depletion in key nodes. UL-VBF (Maximum)'s network lifetime is 16-24% longer than this worst case, demonstrating its capability to maintain network lifetime even under high uncertainty conditions.

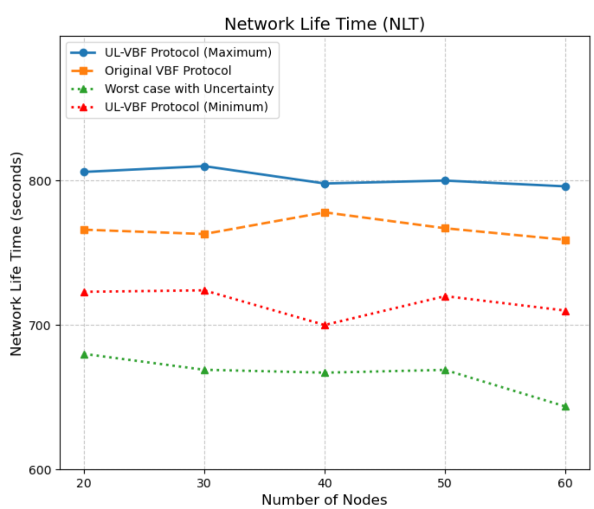

Figure 6: Network Lifetime Comparison

4 Conclusion

This paper presents the UL-VBF protocol, designed to address the challenges of positional uncertainties and energy efficiency in underwater communication networks. Two methods, interval arithmetic and Gurobi optimization are used to solving for accurate values. The tradeoffs are discussed relating to lower and upper bounds and the energy concerns. The evaluations show that UL-VBF performs better than the original VBF protocol in general. Especially, UL-VBF ensures more balance in energy consumption. In the future, enhancements by addressing uncertainty in more underwater AUV network protocols will be conducted.

Acknowledgments

This research is supported by NSF grant CNS-2016726.

References

[1] Götz Alefeld and Günter Mayer. 2000. Interval analysis: theory and applications. *J. Comput. Appl. Math.* 121, 1 (2000), 421–464. https://doi.org/10.1016/S0377-0427(00)00342-3

[2] Ulrich Behrje, Cedric Isokeit, Benjamin Meyer, and Erik Maehle. 2018. A Robust Acoustic-Based Communication Principle for the Navigation of an Underwater Robot Swarm. In *2018 OCEANS - MTS/IEEE Kobe Techno-Oceans (OTO)*. 1–5. https://doi.org/10.1109/OCEANSKOBE.2018.8558871

[3] Paolo Casari, Francesco Ardizzon, and Stefano Tomasin. 2022. Physical Layer Authentication in Underwater Acoustic Networks with Mobile Devices. In *Proceedings of the 16th International Conference on Underwater Networks & Systems* (Boston, MA, USA) *(WUWNet '22)*. Association for Computing Machinery, New York, NY, USA, Article 4, 8 pages. https://doi.org/10.1145/3567600.3567604

[4] Gurobi Optimization, LLC. 2023. Gurobi Optimizer Reference Manual. https://www.gurobi.com

[5] Cedric Isokeit, Benjamin Meyer, and Erik Maehle. 2017. Cooperative swarm behaviour for in situ underwater environmental measurements. In *OCEANS 2017 - Aberdeen*. 1–6. https://doi.org/10.1109/OCEANSE.2017.8084674

[6] Yanting Luo, Yongmin Yang, Shigang Zhang, Xu Luo, and Lei Li. 2020. Performance Analysis and Optimization of The MCR-WPT System with Uncertain Parameters. In *2020 IEEE Wireless Power Transfer Conference (WPTC)*. 154–158. https://doi.org/10.1109/WPTC48563.2020.9295639

[7] Robert Martin, Sanguthevar Rajasekaran, and Zheng Peng. 2017. Aqua-Sim Next Generation: An NS-3 Based Underwater Sensor Network Simulator. In *Proceedings of the 12th International Conference on Underwater Networks & Systems* (Halifax, NS, Canada) *(WUWNet '17)*. Association for Computing Machinery, New York, NY, USA, Article 3, 8 pages. https://doi.org/10.1145/3148675.3148679

[8] Nicolas Nicolaou, Andrew See, Peng Xie, Jun-Hong Cui, and Dario Maggiorini. 2007. Improving the Robustness of Location-Based Routing for Underwater Sensor Networks. In *OCEANS 2007 - Europe*. 1–6. https://doi.org/10.1109/OCEANSE.2007.4302470

[9] Affan A. Syed, Wei Ye, John Heidemann, and Bhaskar Krishnamachari. 2007. Understanding Spatio-Temporal Uncertainty in Medium Access with ALOHA Protocols. In *Proceedings of the 2nd Workshop on Underwater Networks* (Montreal, Quebec, Canada) *(WUWNet '07)*. Association for Computing Machinery, New York, NY, USA, 41–48. https://doi.org/10.1145/1287812.1287822

[10] Xiong Xiao, Xiao Ji, Guang Yang, and Yan Cong. 2012. LE-VBF: Lifetime-Extended Vector-Based Forwarding Routing. *Proceedings - 2012 International Conference on Computer Science and Service System, CSSS 2012*, 1201–1203. https://doi.org/10.1109/CSSS.2012.304

[11] Peng Xie, Jun hong Cui, and Li Lao. 2006. VBF: Vector-Based Forwarding Protocol for Underwater Sensor Networks. In *Networking*. https://api.semanticscholar.org/CorpusID:191949